



Majorana Modes at the Ends of Superconductor Vortices in Doped Topological Insulators

Pavan Hosur,¹ Pouyan Ghaemi,^{1,2} Roger S. K. Mong,¹ and Ashvin Vishwanath^{1,2}

¹*Department of Physics, University of California, Berkeley, California 94720, USA*

²*Materials Sciences Division, Lawrence Berkeley National Laboratory, Berkeley, California 94720, USA*

(Received 24 December 2010; published 22 August 2011)

Recent experiments have observed bulk superconductivity in doped topological insulators. Here we ask whether vortex Majorana zero modes, previously predicted to occur when *s*-wave superconductivity is induced on the surface of topological insulators, survive in these doped systems with metallic normal states. Assuming inversion symmetry, we find that they do but only below a critical doping. The critical doping is tied to a topological phase transition of the vortex line, at which it supports gapless excitations along its length. The critical point depends only on the vortex orientation and a suitably defined SU(2) Berry phase of the normal state Fermi surface. By calculating this phase for available band structures we determine that superconducting *p*-doped Bi₂Te₃, among others, supports vortex end Majorana modes. Surprisingly, superconductors derived from topologically trivial band structures can support Majorana modes too.

DOI: 10.1103/PhysRevLett.107.097001

PACS numbers: 74.25.Uv, 74.25.Dw

Majorana fermions, defined as fermions that are their own antiparticles unlike conventional Dirac fermions such as electrons, have long been sought by high energy physicists, but so far in vain. Of late, the search for Majorana fermions has remarkably shifted to condensed matter systems [1–3], especially, to superconductors (SCs), where states appear in conjugate pairs with equal and opposite energies. Then, a single state at zero energy is its own conjugate and hence, a Majorana state or a Majorana zero mode (MZM). These states are immune to local noise and hence, considered strong candidates for storing quantum information and performing fault tolerant quantum computation [4]. Moreover, they show non-Abelian rather than Bose or Fermi statistics which leads to a number of extraordinary phenomenon [5].

Despite many proposals direct experimental evidence for a MZM is still lacking. While initial proposals involved the $\nu = 5/2$ quantum Hall state and SCs with unconventional pairing such as $p_x + ip_y$ [3], a recent breakthrough occurred with the discovery of topological insulators (TIs) [6], which feature topologically protected metallic surface bands. When a conventional *s*-wave SC is brought near this metallic surface, a single MZM is trapped in the vortex core [7]. Since then, several TIs were found to exhibit bulk superconductivity on doping [8] or under pressure [9,10]. The normal phase of these SCs is now metallic, which raises the question: can a SC vortex host a surface MZM even when the bulk is not insulating?

In this Letter, we answer this question in the affirmative and in the process, discover a convenient way to obtain a MZM, which allows us to conclude that some existing experimental systems should possess these states. Our proposal involves simply passing a magnetic field through a TI-based SC, such as superconducting Bi₂Te₃, in which the doping is below a certain threshold value. We also find

general criteria for SCs to host vortex MZMs and show that some non-TI-based SCs satisfy them too.

A heuristic rule often applied to answer the above question is to examine whether the normal state bulk Fermi surface (FS) is well separated from surface states in the Brillouin zone. If it is, MZMs are assumed to persist in the bulk SC. While this may indicate the presence of low energy states, it is not a topological criterion since it depends on nonuniversal details of surface band structure, and cannot signal the presence of true MZMs. For MZMs to disappear, a gapless channel must open that allows pairs to approach each other and annihilate. We therefore search for and offer a bulk rather than a surface criterion. In this process, we have uncovered the following interesting facts. We assume inversion (\mathcal{I}) and time reversal (\mathcal{T}) symmetric band structures, and weak pairing, since these lead to a technical simplification and capture many real systems. (i) The appearance of surface MZMs is tied to the topological state of the vortex, viewed as a 1D topological SC. The critical point at which they disappear is linked to a vortex phase transition (VPT) where this topology changes. If verified, this may be the first instance of a phase transition inside a topological defect. (ii) The topological state of a vortex depends in general on its orientation. (iii) Symmetry dictates that the normal state FS is doubly degenerate, leading to an SU(2) non-Abelian Berry phase [11] for closed curves, which determines the condition for quantum criticality of the vortex. This is a rare example of a non-Abelian Berry phase directly influencing measurable physical properties of an electronic system. Spin-orbit coupling is essential to obtaining the SU(2) Berry Phase. (iv) Using this criterion and available band structures we find that MZMs occur in *p*-doped superconducting Bi₂Te₃ [10] and in Cu-doped Bi₂Se₃ [8] if the vortex is sufficiently tilted off the *c* axis. *c*-axis

vortices in Cu-doped Bi_2Se_3 are predicted to be near the topological transition.

The problem.—Consider a 3D insulating band structure H , which we dope by changing the chemical potential μ away from the middle of the band gap. Now, add conventional s -wave even parity pairing Δ (in contrast to the odd parity pairing of Ref. [12]) and introduce a single vortex line into the pairing function $\Delta(\mathbf{r})$, stretching between the top and bottom surfaces. We neglect the effect of the magnetic field used to generate the vortices, assuming extreme type II limit. When H is a strong TI, and μ is in the band gap, the pair potential primarily induces superconductivity on the surface states. In this limit it is known [7] that MZMs appear on the surface, in the vortex core [13]. Now consider tuning μ deep into the bulk bands. By modifying states well below μ , one could tune the band structure to one with uninverted bands. One now expects “normal” behavior, and the absence of MZMs. Therefore, a quantum phase transition must occur between these limits at $\mu = \mu_c$.

To understand the nature of the transition, we recall some basic facts of vortex electronic structure, which are also derived below. Once μ enters the bulk bands, low energy Caroli–de Gennes–Matricon excitations appear, bound to the vortex line [14]. These excitations are still typically gapped, although by a small energy scale, the “minigap”: $\delta \sim \Delta/(k_F\xi)$ (where k_F is the Fermi wave vector and ξ is the coherence length. In the weak pairing limit $k_F\xi \gg 1$). This small energy scale arises because the gap vanishes in the vortex core leading to a droplet of normal fluid, which is eventually gapped by the finite vortex size. However, the presence of the minigap is important, since it blocks the tunneling of the surface MZMs into the vortex line, and confines them near the surface. The closing of the minigap allows the surface MZMs to tunnel along the vortex line and annihilate each other.

Vortex as a 1D topological SC.—The VPT may be viewed as a change in the topology of the electronic structure of the vortex line. The relevant energy scale is of the order of the minigap $\delta \ll \Delta$, with excitations localized within the 1D vortex core. The vortex admits particle-hole symmetry (\mathcal{C}) but breaks \mathcal{T} symmetry and hence, belongs to class D of the Altland-Zirnbauer classification [15]. Thus, the problem reduces to classifying gapped phases in 1D within the symmetry class D , which are known to be distinguished by a \mathbb{Z}_2 topological invariant [1]. The two kinds of phases differ in whether they support MZMs at their ends. The topologically nontrivial phase does and hence corresponds to the $\mu < \mu_c$ phase of the vortex line. On raising μ , the vortex line transitions into the trivial phase, via a quantum critical point at which it is gapless along its length. This is reminiscent of recent proposals to generate MZMs at the ends of superconducting quantum wires [16]. Note, since there is no “local” gap in the vortex core, the powerful defect topology classification of [17] cannot be applied.

The Hamiltonian.—The Hamiltonian is $\mathbf{H} = \frac{1}{2} \sum_{\mathbf{k}} \Psi_{\mathbf{k}}^\dagger \mathcal{H}_{\mathbf{k}}^{\text{BdG}} \Psi_{\mathbf{k}}$ where $\Psi_{\mathbf{k}}^\dagger = (\mathbf{c}_{\mathbf{k}\uparrow}^\dagger, \mathbf{c}_{\mathbf{k}\downarrow}^\dagger, \mathbf{c}_{-\mathbf{k}\downarrow}, -\mathbf{c}_{-\mathbf{k}\uparrow})$ and $\mathbf{c}_{\mathbf{k}\sigma}^\dagger$ is assumed to have $a = 1 \dots N$ orbital components $\mathbf{c}_{\mathbf{k}\sigma a}^\dagger$ and

$$\mathcal{H}_{\mathbf{k}}^{\text{BdG}} = \begin{bmatrix} H_{\mathbf{k}} - \mu & \Delta \\ \Delta^* & \mu - H_{\mathbf{k}} \end{bmatrix}, \quad (1)$$

where scalars such as μ and Δ multiply the identity matrix $\mathbf{1}_{2N \times 2N}$. The band Hamiltonian $H_{\mathbf{k}}$ is a $2N \times 2N$ matrix with \mathcal{T} symmetry: $\sigma_y H_{\mathbf{k}}^* \sigma_y = H_{\mathbf{k}}$, where σ_y acts on the spin, which yields the Hamiltonian structure above. When I symmetry is also present, $H_{\mathbf{k}}$ will be doubly degenerate, since the combined operation $\mathcal{T}I$ leads to a Kramers pair at every momentum. $\mathcal{H}_{\mathbf{k}}^{\text{BdG}}$ has particle-hole symmetry implemented by the transformation $\mathcal{C} = \Pi_y \sigma_y \mathcal{K}$, where Π matrices act on Nambu particle-hole indices, and \mathcal{K} denotes complex conjugation. A vortex given by $\Delta(\mathbf{r}) = |\Delta(r)|e^{-i\theta}$, breaks \mathcal{T} but preserves \mathcal{C} .

Role of vortex orientation.—Consider a straight vortex along \hat{z} . The dispersion $\mathcal{E}(k_z)$ in general, has a minigap δ as in Fig. 1. A topological phase transition requires closing of the minigap and reopening with inverted sign. Since the \mathbb{Z}_2 topological index is only changed by an odd number of such band crossings, the only relevant momenta are $k_z = 0, \pi$. Band touchings at other k_z points occur in pairs at $\pm k_z$ which do not alter the \mathbb{Z}_2 index [1]. In the weak pairing limit, one expects the critical point μ_c to be determined by a FS property, which will be outlined in detail below. Here we simply observe that the relevant FSs to consider lie in the $k_z = 0, \pi$ planes, the planes determined by the vortex orientation. This implies that the topological phase of the vortex, and hence μ_c , depend in general on its orientation.

VPT in a lattice model.—Before discussing the general criterion for a VPT, we present numerical and analytical evidence in a specific lattice model from Ref. [18]. While the numerics explicitly demonstrate the phase transition, the analytical treatment of the continuum limit allows us to conjecture a Berry phase condition for the transition, which is later proved. The model is on a simple cubic lattice with two orbitals per site: $H_{\mathbf{k}}^{\text{att}} = \tau_x \mathbf{d}_{\mathbf{k}} \cdot \boldsymbol{\sigma} + m_{\mathbf{k}} \tau_z - \mu$ where τ_i (σ_i) are Pauli matrices in the orbital (spin) basis, $d_{\mathbf{k}}^i = 2t \sin k_i$, $m_{\mathbf{k}} = (M + m_0 \sum_i \cos k_i)$, $i = x, y, z$, and t , m_0 , and M are parameters of the model and μ is the chemical potential. The model is in the strong TI phase if $-3 < \frac{M}{m_0} < -1$. We add a mean field s -wave pairing to this Hamiltonian, insert a unit winding into the pairing function, and diagonalize the Hamiltonian numerically. We focus on $k_z = 0$.

Numerical results.—Figure 1 illustrates the evolution of the bulk vortex bound states, the dispersion within the vortex, and the surface MZMs as a function of μ , when the normal state has a band inversion only at the $\Gamma = (0, 0, 0)$ point, i.e., $m_{\Gamma} < 0$. At $\mu = 0$, the bulk is

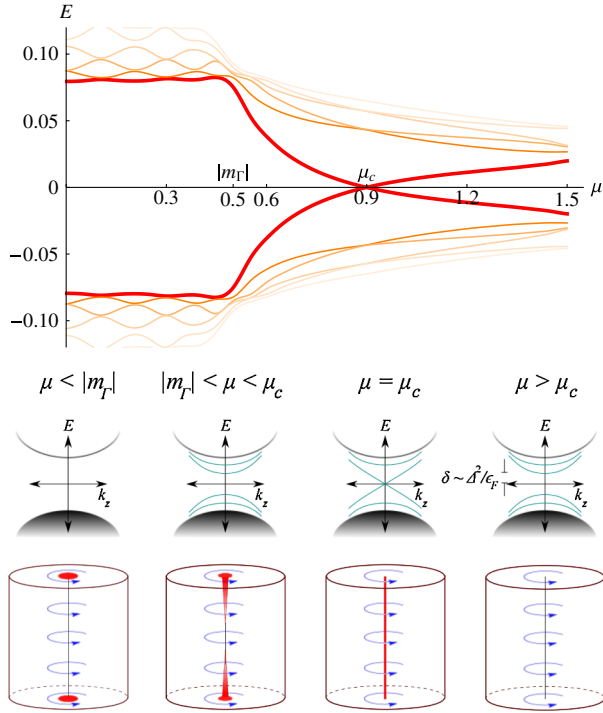


FIG. 1 (color online). The vortex phase transition. Evolution of the lowest few states at $k_z = 0$ (top row), of the dispersion within the vortex (middle row) and of the surface MZMs (bottom row) as μ is varied when the normal phase has a band inversion at Γ . At $\mu = 0$, the normal phase is a strong TI and a superconducting vortex traps a MZM at its ends. As μ is increased, it first enters the conduction band at $\mu = |m_\Gamma|$ and midgap states appear inside the vortex. For $\mu < \mu_c$, the vortex stays gapped, but with a minigap δ smaller than the bulk gap. The MZMs remain trapped near the surface. At $\mu_c = 0.9$, the gap vanishes signaling a phase transition. Beyond μ_c , the vortex is gapped again, but there are no surface MZMs. We used the lattice Hamiltonian with the parameters $t = 0.5$, $M = 2.5$, and $m_0 = -1.0$. The pairing strength is $\Delta_0 = 0.1$ far away from the vortex and drops sharply to zero at the core. Other gap profiles give similar results.

gapped and must have a pair of MZMs on opposite surfaces in a slab geometry. As μ is raised, these MZMs leak deeper into the bulk, but survive even after μ crosses $|m_\Gamma|$ despite the bulk now having a FS in the normal phase, gapped by superconductivity. A VPT eventually occurs at $\mu_c = 0.9$, at which the vortex is gapless and the surface MZMs merge into vortex line. Beyond μ_c , there are no longer any protected MZMs on the surface.

Continuum limit.—In the continuum limit of the lattice model, we can analytically calculate μ_c . For $k_z = 0$ and small $k_{x,y}$ around Γ , $H_{\mathbf{k}}^{\text{latt}}$ reduces to the isotropic form $\mathcal{H}_{\mathbf{k}} = v_D \tau_x \boldsymbol{\sigma} \cdot \mathbf{k} + (m - \epsilon k^2) \tau_z - \mu$. In this form, a band inversion exists if $m\epsilon > 0$. Thus, $m\epsilon < 0$ (> 0) defines a trivial insulator (strong TI). At $k = \sqrt{m/\epsilon}$, $m_{\mathbf{k}} = m - \epsilon k^2$ vanishes and $\mathcal{H}_{\mathbf{k}}$ resembles two copies of a TI surface. In particular, the Berry phase around each

$\tau_x = \pm 1$ FS is π . We show later that this leads to a pair of vortex zero modes, signaling the VPT at $\mu_c = v_D \sqrt{m/\epsilon}$.

We solve analytically for the two bulk zero modes at μ to first order in Δ_0 assuming $|\Delta(\mathbf{r})| = \Delta_0 \Theta(r - R)$, where Θ is the step function and $\mu R / v_D \gg 1$. Calculating the zero modes separately for $r \leq R$ and $r \geq R$ and matching the solutions at $r = R$ gives a pair of zero modes, only when $\mu = v_D \sqrt{m/\epsilon}$, for all vortex orientations. This is precisely where the momentum dependent “mass” term changes sign [19]. Using the model parameters and the linearized approximation gives an estimate of $\mu_c \approx 1$, in agreement with the lattice numerics.

General Fermi surface Berry phase condition.—For weak pairing, the VPT is expected to be governed by properties of the bulk FS. For concreteness, we begin by assuming we have a single FS in the $k_z = 0$ plane, which will be doubly degenerate due to the combined symmetry $\mathcal{T}I$. We now argue that the VPT occurs when an appropriately defined Berry phase for each of the two degenerate bulk FSs is π .

A convenient model for the vortex is $\Delta(\mathbf{r}) = \frac{\Delta_0}{\xi}(x - iy)$. The linear profile here simplifies calculations, but does not affect the location of the zero mode. The choice of ξ as the length scale gives the right minigap scale for the low energy excitations. Working in momentum space, we substitute \mathbf{r} by $i\partial_{\mathbf{k}}$, which gives

$$\mathcal{H}_{\mathbf{k}}^{\text{BdG}} = \begin{bmatrix} H_{\mathbf{k}} - \mu & i \frac{\Delta_0}{\xi} (\partial_{k_x} - i \partial_{k_y}) \\ i \frac{\Delta_0}{\xi} (\partial_{k_x} + i \partial_{k_y}) & \mu - H_{\mathbf{k}} \end{bmatrix}, \quad (2)$$

transforming now to the band basis $|\varphi_{\mathbf{k}}^\nu\rangle$, which are eigenstates of the band Hamiltonian $H_{\mathbf{k}}|\varphi_{\mathbf{k}}\rangle = E_{\mathbf{k}}|\varphi_{\mathbf{k}}\rangle$. Since we are only interested in very low energy phenomena, we project onto the two degenerate bands near the Fermi energy $\nu = 1, 2$. The projected Hamiltonian then is

$$\tilde{\mathcal{H}}_{\mathbf{k}}^{\text{BdG}} = \begin{bmatrix} E_{\mathbf{k}} - \mu & i \frac{\Delta_0}{\xi} (D_{k_x} - i D_{k_y}) \\ i \frac{\Delta_0}{\xi} (D_{k_x} + i D_{k_y}) & -E_{\mathbf{k}} + \mu \end{bmatrix}, \quad (3)$$

where $D_{k_\alpha} = \partial_{k_\alpha} - i\mathbf{A}_\alpha(\mathbf{k})$ and $\mathbf{A}_\alpha(\mathbf{k})$, the $SU(2)$ connections, are 2×2 matrices: $[\mathbf{A}]_{\alpha}^{\mu\nu}(\mathbf{k}) = i\langle \varphi_{\mathbf{k}}^\mu | \partial_{k_\alpha} | \varphi_{\mathbf{k}}^\nu \rangle$.

(i) *Abelian case.*—Let us first consider the case when an additional quantum number (such as spin) can be used to label the degenerate FSs. Then, $[\mathbf{A}]_{\alpha}^{\mu\nu}$ must be diagonal, and reduces to a pair of $U(1)$ connections for the two FSs. In this situation, (3) is identical to the effective Hamiltonian for a $p_x + ip_y$ SC, if we interpret momenta as position and ignore the gauge potential. The diagonal terms represent a transition from weak to strong pairing phase on crossing the FS when $E_{\mathbf{k}} = \mu$ [3]. Thus midgap states are expected, composed of states near the Fermi energy. Because of the finite size of the FS, these states have an energy spacing of $\mathcal{O}(\frac{\Delta_0}{k_F \xi})$, the minigap energy scale. However, a zero energy state appears if the FS

encloses a π flux [3]. This can be implemented via the gauge potential if $\oint_{\text{FS}} \mathbf{A} \cdot d\mathbf{l} = \pi$ leading to a pair of zero modes, since the other FS has the same Berry phase by \mathcal{T} .

(ii) *General case, SU(2) connection.*—In the absence of any quantum number distinguishing the bands, one integrates the vector potential $\mathbf{A}(\mathbf{k})$ around the FS in the $k_z = 0$ plane, to obtain the non-Abelian Berry phase $U_B = \mathcal{P} \exp[i \oint_{\text{FS}} \mathbf{A} \cdot d\mathbf{l}] \in \text{SU}(2)$, where \mathcal{P} denotes path ordering. [There is no U(1) phase by \mathcal{T} symmetry.] Although U_B itself depends on the choice of basis, its eigenvalues $e^{\pm i\phi_B}$ are gauge invariant. A semiclassical analysis [19] gives the Bohr-Sommerfeld type quantization condition for the low energy levels:

$$E_n = \frac{\Delta_0}{l_F \xi} (2\pi n + \pi \pm \phi_B), \quad (4)$$

where n is an integer and l_F is the FS perimeter. A pair of zero modes appears when $\phi_B = \pi$, i.e., when $U_B = -1$.

We have considered a single closed FS in the $k_z = 0$ plane. Such a FS necessarily encloses a \mathcal{T} invariant momentum (TRIM), (e.g., Γ), given the symmetries. When there are multiple FSs, the condition above is applied individually to each FS, since tunneling between them is neglected in the semiclassical approximation. Closed FSs that do not enclose a TRIM, or pairs of open FSs, cannot change the vortex topology.

Candidate materials.—We now apply the Berry phase criterion to some candidate materials to see which of them can have protected MZMs at the ends of vortices.

$\text{Cu}_x\text{Bi}_2\text{Se}_3$.—The insulating phase of Bi_2Se_3 is a strong TI with a single band inversion occurring at the Γ point. On Cu doping, Bi_2Se_3 becomes n type with an electron pocket at Γ and is reported to superconduct below $T_c = 3.8$ K [8,20]. Photoemission measurements show $\mu \approx 0.25$ eV above the conduction band minimum at optimal doping [21]. We calculate the Berry phase eigenvalues for a FS around the Γ point numerically as a function of μ , which evaluates to $\pm\pi$ at $\mu_c \approx 0.24$ eV above the conduction band minimum for a vortex along the c axis of the crystal [19]. Hence $\mu \gtrsim \mu_c$ indicates c -axis vortices are near the topological transition. However, tilting the vortex away from the c axis is found to raise μ_c to up to $\mu_c = 0.30$ eV, for a vortex perpendicular to the c axis. Therefore, sufficiently tilted vortices should host MZMs at the experimental doping level.

p-doped TlBiTe₂, p-doped Bi₂Te₃ under pressure and Pd_xBi₂Te₃.—The bands of TlBiTe₂ and Bi₂Te₃ are topologically nontrivial because of a band inversion at the Γ point [22]. The topological character of Bi₂Te₃ is believed to be preserved under a pressure of up to 6.3 GPa, at which it undergoes a structural phase transition. On p doping to a density of $6 \times 10^{20} \text{ cm}^{-3}$ ($3\text{--}6 \times 10^{18} \text{ cm}^{-3}$), TlBiTe₂ (Bi₂Te₃ under 3.1 GPa) becomes a SC below $T_c = 0.14$ K (~ 3 K) [10,23], making it a natural system to search for the possibility of MZMs. Similarly, n -doping

Bi₂Te₃ to a concentration of $9 \times 10^{18} \text{ cm}^{-3}$ by adding Pd reportedly results in $T_c = 5.5$ K [8] in a small sample fraction. The superconductivity in Bi₂Te₃ under pressure, and in TlBiTe₂ (Pd_xBi₂Te₃) is believed to arise from six symmetry related hole (electron) pockets around the Γ -T line. This is an even number so vortex lines in superconducting TlBiTe₂ and both p - and n -type Bi₂Te₃ should have MZMs at their ends in all orientations.

MZMs from trivial insulators.—The bulk criterion derived does not require a “parent” topological band structure. As a thought example, say we have four TRIMs with Hamiltonians like the continuum Hamiltonian $\mathcal{H}_{\mathbf{k}}$ in their vicinity. Such band inversions at four TRIMs in a plane leads to a trivial insulator [24]. However, if their critical chemical potentials μ_c differ, then there could be a range of μ where there are an odd number of VPTs below and above μ , leading to topologically nontrivial vortices. Interestingly PbTe and SnTe are both trivial insulators with band inversions relative to each other at the four equivalent L points. They both exhibit superconductivity on doping below $T_c = 1.5$ K [25] and 0.2 K [26], respectively. A combination of strain (to break the equivalence of the four L points) and doping could potentially create the scenario described above in one of these systems. GeTe is similar to SnTe with $T_c \sim 0.3$ K [27] but undergoes a spontaneous rhombohedral distortion resulting in the desired symmetry. Thus, I - and \mathcal{T} -symmetric systems with strong spin orbit can lead to SCs with vortex end MZMs, even in the absence of a proximate topological phase. Investigating the Fermi surface SU(2) Berry phases, and thus the vortex electronic structure, in this wide class of systems is a promising future direction in the hunt for Majorana fermions.

In closing, we note that the VPT could potentially be probed via thermal transport along the vortex line. A hurdle is the small minigap scale ($\Delta/k_F \xi \sim \Delta^2/E_F$), and the long confinement length of the MZMs to the surface, which may be ameliorated by considering strong coupling SCs or materials such as heavy fermions where E_F is reduced.

We thank A. M. Turner, J. H. Bardarson, A. Wray, and C. L. Kane for insightful discussions, and NSF-DMR 0645691 for funding. In parallel work, L. Fu, J. C. Y. Teo, and C. L. Kane have arrived at similar conclusions.

-
- [1] A. Y. Kitaev, *Phys. Usp.* **44**, 131 (2001).
 - [2] S. Das Sarma, C. Nayak, and S. Tewari, *Phys. Rev. B* **73**, 220502 (2006).
 - [3] N. Read and D. Green, *Phys. Rev. B* **61**, 10267 (2000).
 - [4] Nayak *et al.*, *Rev. Mod. Phys.* **80**, 1083 (2008).
 - [5] G. Moore and N. Read, *Nucl. Phys.* **B360**, 362 (1991).
 - [6] M. Z. Hasan and C. L. Kane, *Rev. Mod. Phys.* **82**, 3045 (2010); X. L. Qi and S. C. Zhang, arXiv:1008.2026; M. Z. Hasan and J. E. Moore, *I Annu. Rev. Condens. Matter Phys.* **2**, 55 (2011).
 - [7] L. Fu and C. L. Kane, *Phys. Rev. Lett.* **100**, 096407 (2008).

- [8] Y. S. Hor *et al.*, *J. Phys. Chem. Solids* **72**, 572 (2011).
- [9] M. Einaga *et al.*, *J. Phys. Conf. Ser.* **215**, 012036 (2010).
- [10] J.L. Zhang *et al.*, *Proc. Natl. Acad. Sci. U.S.A.* **108**, 24 (2011).
- [11] F. Wilczek and A. Zee, *Phys. Rev. Lett.* **52**, 2111 (1984).
- [12] L. Fu and E. Berg, *Phys. Rev. Lett.* **105**, 097001 (2010).
- [13] It is convenient to discuss pairing over the entire range of μ , using the mean field Hamiltonian (1), although in reality superconductivity only appears once bulk carriers are induced.
- [14] C. Caroli, P.G. de Gennes, and J. Matricon, *Phys. Lett.* **9**, 307 (1964).
- [15] A. Altland and M.R. Zirnbauer, *Phys. Rev. B* **55**, 1142 (1997).
- [16] R.M. Lutchyn, J.D. Sau, and S. Das Sarma, *Phys. Rev. Lett.* **105**, 077001 (2010); Y. Oreg, G. Refael, and F. von Oppen, *ibid.* **105**, 177002 (2010); M. Wimmer *et al.*, *ibid.* **105**, 046803 (2010); A. C. Potter and P. A. Lee, *ibid.* **105**, 227003 (2010).
- [17] J.C.Y. Teo and C.L. Kane, *Phys. Rev. B* **82**, 115120 (2010).
- [18] P. Hosur, S. Ryu, and A. Vishwanath, *Phys. Rev. B* **81**, 045120 (2010).
- [19] See Supplemental Material at <http://link.aps.org/supplemental/10.1103/PhysRevLett.107.097001> for further details of the calculation.
- [20] Y. S. Hor *et al.*, *Phys. Rev. Lett.* **104**, 057001 (2010).
- [21] L. A. Wray *et al.*, *Nature Phys.* **6**, 855 (2010).
- [22] B. Yan *et al.*, *Europhys. Lett.* **90**, 37002 (2010); H. Lin *et al.*, *Phys. Rev. Lett.* **105**, 036404 (2010); S. Eremeev, Y. Koroteev, and E. Chulkov, *JETP Lett.* **91**, 594 (2010); Y. Chen *et al.*, *Phys. Rev. Lett.* **105**, 266401 (2010); Y. L. Chen *et al.*, *Science* **325**, 178 (2009); H. Zhang *et al.*, *Nature Phys.* **5**, 438 (2009).
- [23] R. A. Hein and E. M. Swiggard, *Phys. Rev. Lett.* **24**, 53 (1970).
- [24] L. Fu and C.L. Kane, *Phys. Rev. B* **76**, 045302 (2007).
- [25] Y. Matsushita *et al.*, *Phys. Rev. B* **74**, 134512 (2006).
- [26] R. Hein, *Phys. Lett.* **23**, 435 (1966).
- [27] R. A. Hein *et al.*, *Phys. Rev. Lett.* **12**, 320 (1964).